Supporting Information

Ion exchange biomaterials to capture daptomycin and prevent resistance evolution in off-target bacterial populations

*Shang-Lin Yeh,[1] Naveen Narasimhalu,[1] Landon G. vom Steeg,[2] Joy Muthami,[1] Sean LeConey,[1] Zeming He,[1] Mica Pitcher,[1,3] Harrison Cassady,[4] Valerie J. Morley,[2,+] Sung Hyun Cho,[5] Carol Bator,[5] Roya Koshani,[1] Robert J. Woods,[6] Michael Hickner,[1,4] Andrew F. Read,[2,5] Amir Sheikhi[1,7]**

[1]Department of Chemical Engineering, The Pennsylvania State University, University Park, PA 16802, USA

[2]Department of Biology, The Pennsylvania State University, University Park, PA 16802, USA

[3]Department of Chemistry, The Pennsylvania State University, University Park, PA 16802, USA

[4]Department of Materials Science and Engineering, The Pennsylvania State University, University Park, PA 16802, USA

[5]Huck Institutes of the Life Sciences, The Pennsylvania State University, University Park, PA 16802, USA

[6]Department of Internal Medicine, University of Michigan, Ann Arbor, MI 48109, USA

[7]Department of Biomedical Engineering, The Pennsylvania State University, University Park, PA 16802, USA

[+]Present address: NTx, 7701 Innovation Way, NE Rio Rancho, NM 87144

*Corresponding Author: Amir Sheikhi (sheikhi@psu.edu)

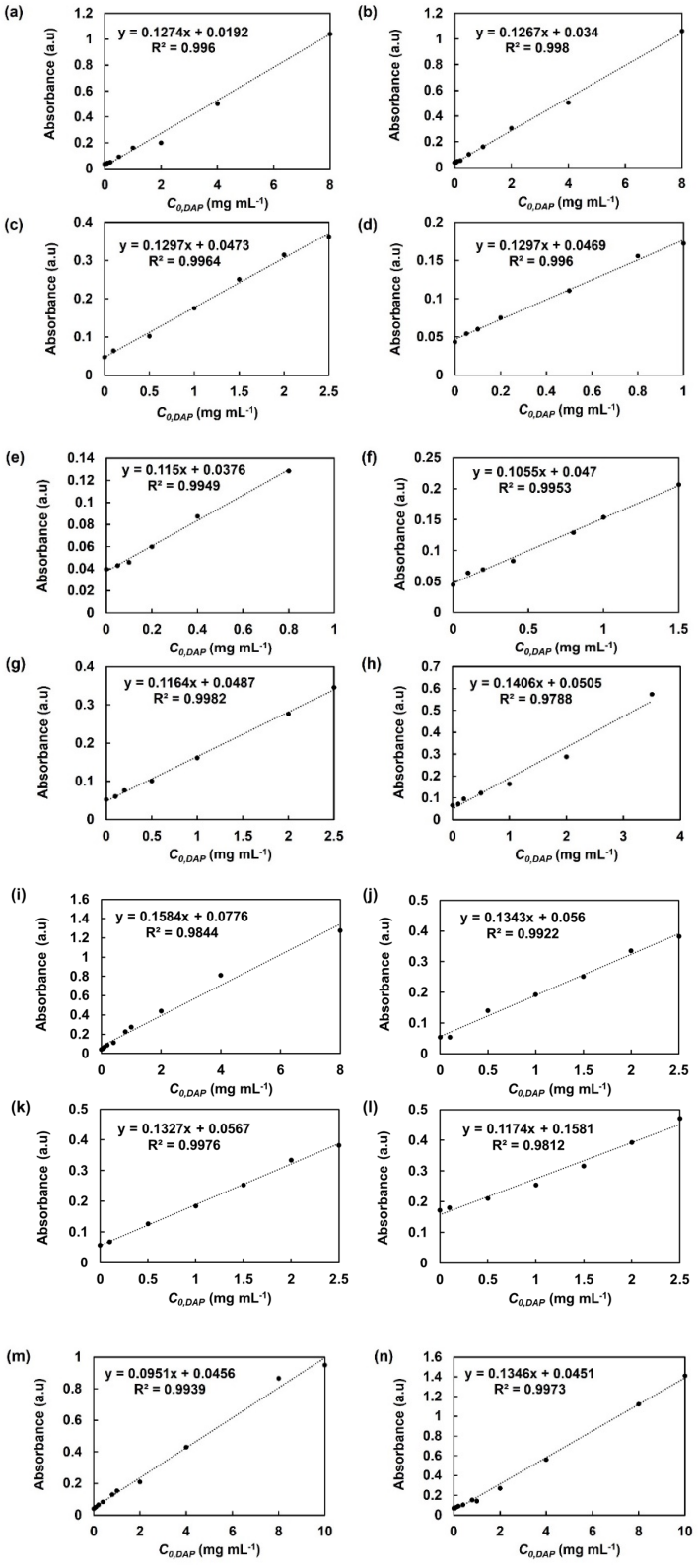

Figure S1. Calibration lines of DAP UV-vis absorbance at 364 nm in **(a)** Milli-Q water,

(b) NaCl solution (500 mM), **(c)** maleic acid (100 mM), **(d)** bile acid (12 mM), and $CaCl_2$ solutions of **(e)** 10 mM, **(f)** 50 mM, **(g)** 100 mM, **(h)** 200 mM, and **(i)** 500 mM, and lecithin solution of **(j)** 0.5 mM, **(k)** 1 mM, and **(l)** 1 mM containing 4 mM of $CaCl_2$, as well as in the **(m)** FaSSIF and **(n)** FeSSIF.

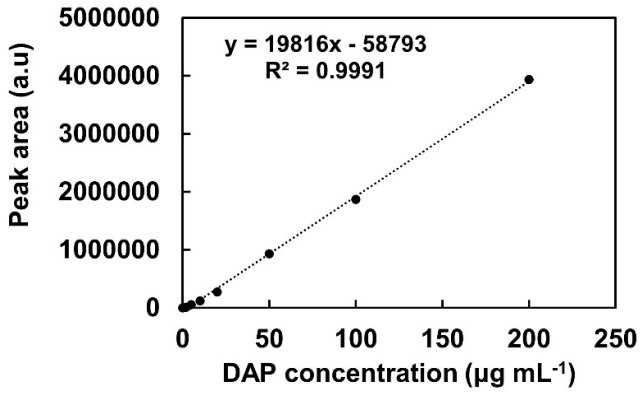

Figure S2. Linear regression analysis of calibration line for DAP solutions, ranging from 10 µg mL^{-1} to 200 µg mL^{-1} in Milli-Q water obtained using the HPLC.

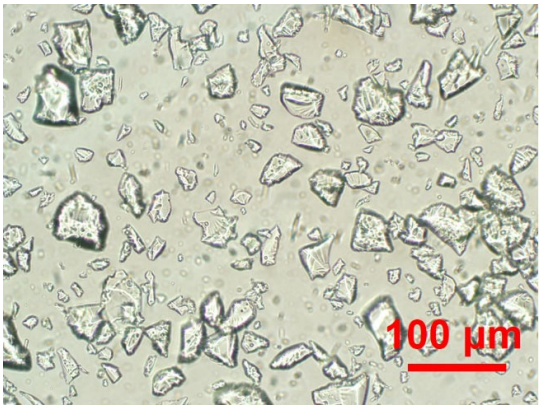

Figure S3. Optical microscopy image of cholestyramine IXB.

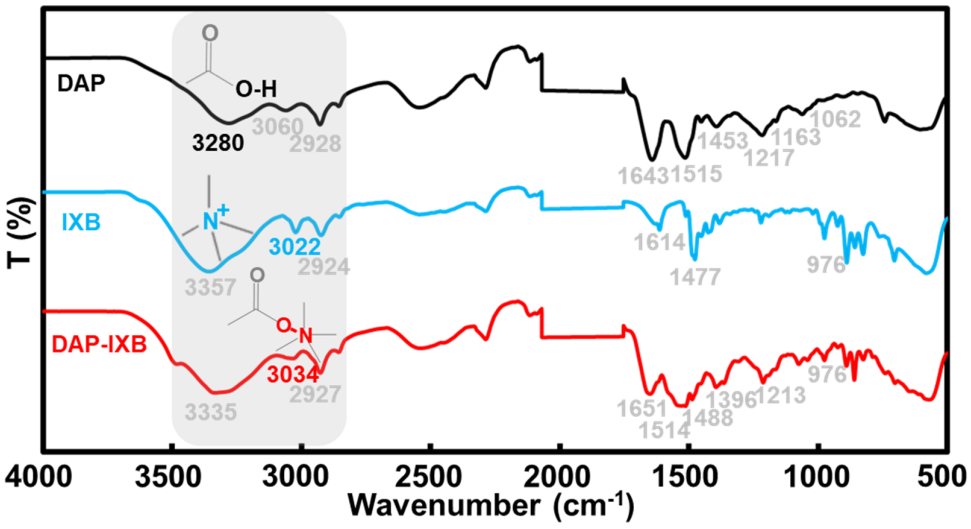

Figure S4. ATR-FTIR spectra of DAP, IXB, and DAP-IXB complex.

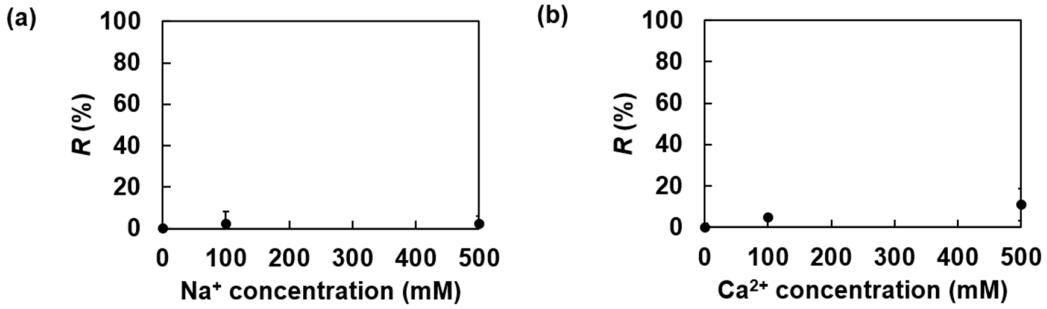

Figure S5. DAP (8 mg mL^{-1}) removal percentage (precipitation) at varying **(a)** Na^{+} and **(b)** Ca^{2+} concentrations without using the IXB. Data are reported as mean ± standard deviation, $n = 3$.

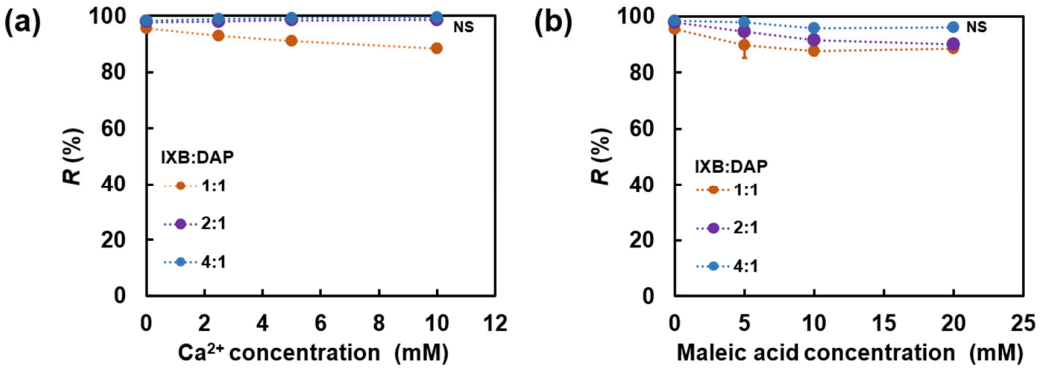

Figure S6. Effect of IXB dose (8, 16, or 32 mg mL^{-1}) on the DAP (8 mg mL^{-1}) removal percentage (R) at varying Ca^{2+} and maleic acid concentrations. Data are presented as mean ± standard deviation, n = 3. NS represents $p>0.05$ for the DAP removal percentage at 10 mM of Ca^{2+} or 20 mM of maleic acid compared with the Ca^{2+}- or maleic acid-free systems, respectively.

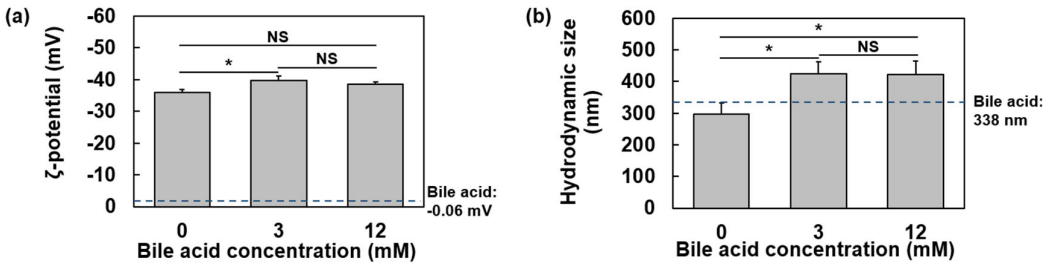

Figure S7. (a) ζ-potential and **(b)** hydrodynamic size of DAP at varying bile acid concentrations. Data are reported as mean ± standard deviation, $n = 3$. NS shows $p>0.05$, * is $p<0.05$, ** represents $p < 0.01$, and *** indicates $p < 0.001$.

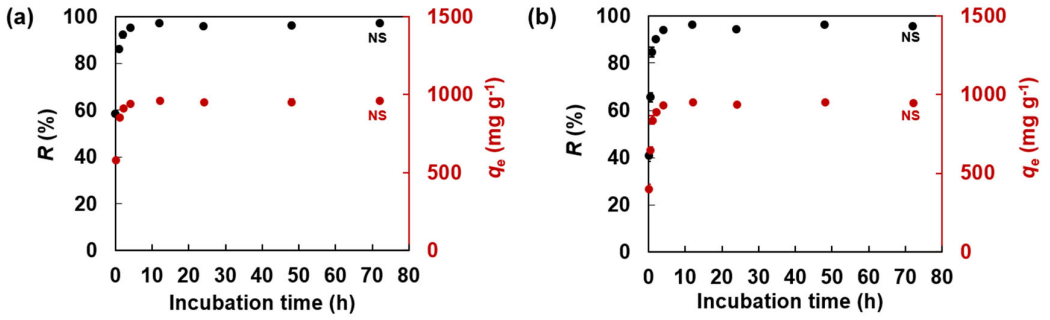

Figure S8. Kinetics of DAP (8 mg mL^{-1}) removal by IXB (8 mg) in the **(a)** FaSSIF or **(b)** FeSSIF. Data are reported as mean ± standard deviation, n = 3. NS represents p>0.05 between the DAP removal percentage or capacity after 4 h or 12 h incubation.

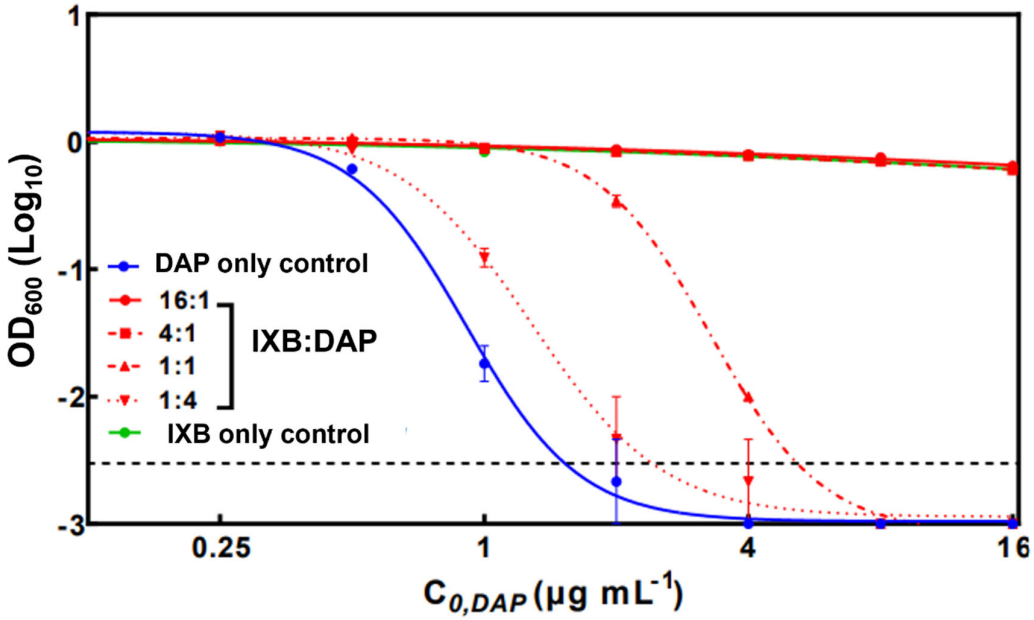

Figure S9. Bacterial densities (OD_{600}) for DAP (256 µg mL^{-1}) after contact with varying doses of cholestyramine IXB. Data are presented as mean ± standard deviation, $n = 4$.